CONSTRUCTION OF AMPEROMETRIC LACCASE-BASED BIOSENSORS USING THE UREASIL AND PHOTOCROSS-LINKED POLYMERS

Taras S. Kavetskyy[1,2,3*], Yuliia Y. Kukhazh[1,3], Khrystyna V. Zubrytska[1,3], Rovshan I. Khalilov[3,4,5], Oleh V. Smutok[1,3,6], Olha M. Demkiv[1,3,6], Ondrej Šauša[7], Helena Švajdlenková[8], Mykhailo V. Gonchar[1,3,6]

[1]Drohobych Ivan Franko State Pedagogical University, Drohobych, Ukraine
[2]The John Paul II Catholic University of Lublin, Lublin, Poland
[3]Joint Ukraine-Azerbaijan International Research and Education Center of Nanobiotechnology and Functional Nanosystems, Drohobych, Ukraine & Baku, Azerbaijan
[4]Baku State University, Baku, Azerbaijan
[5]Institute of Radiation Problems, National Academy of Sciences of Azerbaijan, Baku, Azerbaijan
[6]Institute of Cell Biology, National Academy of Science of Ukraine, Lviv, Ukraine
[7]Institute of Physics, Slovak Academy of Sciences, Bratislava, Slovakia
[8]Polymer Institute, Slovak Academy of Sciences, Bratislava, Slovakia

Abstract. Amperometric laccase-based biosensors of the third generation for analysis of phenol derivates were constructed using the ureasil and photocross-linked polymers as a holding matrix. The knowledge of the properties of the microstructure of such polymer materials is important in terms of optimizing the regulated properties of the amperometric biosensors. Positron annihilation lifetime spectroscopy is a progressive method for microstructural analysis of macromolecular structures. A swelling test provides information about a crosslink density of polymer network. Combination of these both methods allowed to get information about network properties of the polymer matrixes and the results obtained were further compared with sensitivity of bioelectrodes constructed using the polymer matrixes. A role of free-volume and crosslink density in the host polymer matrixes used for improvement of amperometric laccase-based biosensors was established.

1.   Introduction

Technogenic pressure on the environment significantly affects the pollution of water resources. The one of the most dangerous pollutants of wastewater are xenoestrogens. They are a matter of industrial origin in the human body, capable of causing effects similar to the effects of high doses of a natural hormone estrogen (Danzo, 1998; Roy *et al*., 2009). Mimicking estrogen, they adversely affect the function of the endocrine system and able to cause various health defects, affecting synthesis, metabolism and cellular reactions of natural estrogens (Rozati *et al*., 2002; Patisaul &

Adewale, 2009; Watson *et al.*, 2011). Xenoestrogens are a common pollution. They arrive in the surface water with drains of oil, shale, forest-chemical, and cox-chemical industries as well as with drains of hydrolysis industry. For example, xenoestrogen Bisphenol A is a monomer that is used for the manufacture of polycarbonate plastic and epoxy resins, which are raw materials for the production of packaging materials for food and drinks. World market of Bisphenol A is over 6.4 billion pounds per year, and thus, it is one of the chemicals with the highest volume of production all over the world (vom Saal & Hughes, 2005). As a result of hydrolysis of the ester linkages in these polymers, Bisphenol A is released in the environment, resulting in widespread negative impact on human and animals. A list of substances with an endocrine activity is constantly expanding. It includes chlorine-organic and poly-aromatic compounds, the source of which is a plastic used for packaging of drinking water (Oehlmann & Schulte-Oehlmann, 2003), and some pharmaceutical drugs widely used, such as Ibuprofen, in dangerous concentrations. When using Ibuprofen in the order of hundreds of thousands of tons (Germany), the anti-inflammatory drug and its metabolites are detected in all samples of wastewater and sea water at a concentration from 0.1 to 20 µg/L (Contardo-Jara *et al.*, 2011). The main sources of substances with xenoestrogenic effect are the wastewater of cities and animal complexes. A high content of estrogens and pharmaceutical drugs is still existed even after treatment of water (Zhou *et al.*, 2012). Xenoestrogens, classified as carcinogens, are toxic to healthy compounds that cause disruption of the endocrine system of human and animals. The development of new approaches for monitoring of these dangerous substances coming from the wastewater is a topical problem to improve human life first of all. One of such innovations is creation of highly sensitive biosensors for analysis of the level of wastewater pollution.

The commercial laccase can be used in the role of catalytic bioselective element of amperometric biosensor sensitive to different aromatic phenols and amines as a part of the project. Laccase (EC 1.10.3.2 *p*-diphenol: benzenediol oxygen oxidoreductase from *Trametes versicolor*) is a copper containing enzyme which is able to catalyze the oxidation of several phenolic compounds and aromatic amines (Giardina *et al.*, 2010). In a typical laccase reaction, a phenolic substrate is exposed to a single electronic oxidation with the formation of aril radical that in the next stage of the enzymatic reaction is converted into a quinone. Laccase does not need a hydrogen peroxide in the role of co-substrate or additional cofactors for fermentation reaction that makes it an extremely perspective in fabrication of biosensors for monitoring an amount of phenol containing compounds, including some xenoestrogens. Concerning the laccase application for the targeted oxidation of phenolics, the development of biocatalysts application which are stable under environmental condition is a critical issue, which is currently addressed by many work initiatives at EU level, e.g. Knowledge Based Bio Economy (KBBE) programme. Moreover, efficiency of usage laccase form *Trametes versicolor* for effectively removal of C-bisphenol A and C-sodium diclofenac from secondary effluent from a municipal wastewater was demonstrated recently (Arca-Ramos *et al.*, 2016).

Recently, innovative amperometric biosensors for monitoring the level of wastewater pollution have been constructed (Kavetskyy *et al.*, 2017b) on the surface of the gold planar electrodes C220AT "DropSens" by using the organic-inorganic ureasil-based composites as host polymer matrices and immobilized commercial laccase from *Trametes versicolor*. In fact, urea-silicates or ureasils are well-known as representatives of organic-inorganic hybrid polymer materials successfully examined as dispersion

media for luminescent Eu^{3+} salts (Sá Ferreira *et al*., 2001), ion conducting Li^+ salts (de Zea Bermudez *et al*., 1999), organic dyes (Stathatos *et al*., 2000), semiconductor and metal nanoparticles (Boev *et al*., 2004; Boev *et al*., 2006; Kavetskyy *et al*., 2012; Kavetskyy *et al*., 2013), and, for the first time, the ureasil-based composites were tested for immobilization of laccase and construction of biosensors (Kavetskyy *et al*., 2017b). It has been found that the biosensor based on the ureasil-chalcogenide glass composite was characterized by very high sensitivity to be 38.3 times higher in compare with pure ureasil. On the other hand, application of the ureasil-chalcogenide glass composite with incorporated silver nanoparticles synthesized by high-dose 30 keV Ag^+ ion implantation results in decreasing the biosensor sensitivity up to 2390 times. The results obtained indicated a well expressed influence on the sensor's characteristics of the constructed biosensor by organic-inorganic ureasil-based matrixes and silver nanoparticles.

Laccase-based amperometric enzyme biosensors of the third generation for analysis of phenol derivates have also been constructed (Kavetskyy *et al*., 2019) using graphite rods (type RW001) as working electrodes and the photocross-linked polymers as a matrix. Such matrix consisted of epoxidized linseed oil (ELO), bisphenol A diglycidyl ether (RD) as reactive diluent and 50% mixture of triarylsulfonium hexafluorophosphate in propylene carbonate (PI) as photoinitiator. The synthesis was made by the reaction of ELO and 10 mol.% or 30 mol.% of RD, using 3 mol.% of PI (ELO/10RD and ELO/30RD, respectively). The holding matrixes were used for an immobilization of commercial laccase from the fungus *Trametes versicolor*.

In the present work, the results obtained with help of positron annihilation lifetime spectroscopy (PALS) and swelling test are presented for the ureasil-based and photocross-linked polymers used for construction of laccase-based amperometric biosensors. A correlation between the constructed biosensor parameters and microscopical free volume of the biosensor holding matrixes was established.

2.   Experimental

The pure organic-inorganic hybrid ureasil matrix was synthesized as follows (Kavetskyy *et al*., 2012; Kavetskyy *et al*., 2013): O,O'-bis(2-aminopropyl)-polypropylene glycol-block-polyethylene glycol-block-polypropylene glycol-500 (Jeffamine ED-600) was dried under vacuum for 30 minutes; 3-isocyanatepropyltriethoxysilane (ICPTES), tetraethoxysilane (TEOS, 98%) and n-butyl amine was used as received; Jeffamine and ICPTES were mixed in a stoichiometric ratio of 1:2 in order to obtain a liquid ureasilicate monomer; thereafter, TEOS (1.12 mmol) and n-butylamine were added to the mixture, which was kept under stirring for more than 20 min. The mixture was then transferred into a plastic Petri dish and jellified under appropriate conditions; the obtained gels were heated in a vacuum furnace at 333 K at ambient conditions; and a non-rigid, homogeneous and highly transparent xerogel in form of a disk with a diameter of 40 mm and a thickness of 0.25 mm was obtained within 1 day.

At the same time, the organic-inorganic hybrid ureasil matrix with chalcogenide clusters represented by ureasil-chalcogenide glass As_2S_3 composite was synthesized as follows (Kavetskyy *et al*., 2012; Kavetskyy *et al*., 2013): the As_2S_3 ingots were synthesized by melt quenching method from As (5N) and S (5N) in sealed quartz ampoules at 923 K; the melt was quenched to room temperature, and the obtained glassy samples were finely grounded in powder form and dissolved in an organic
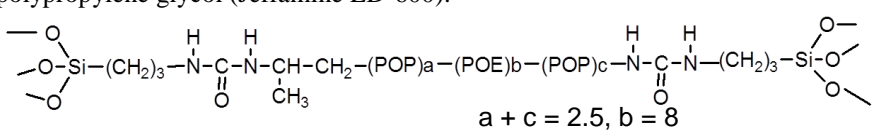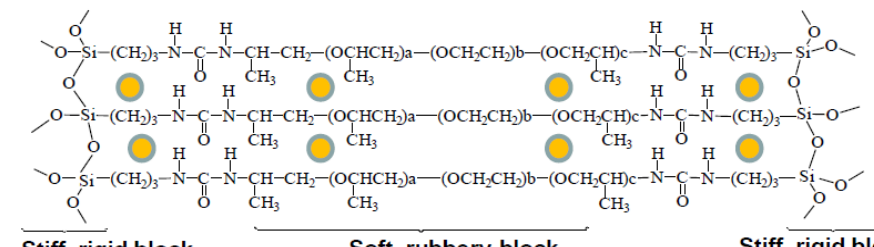
solvent (3 ml n-butylamine) to the 0.4 M concentration; and the ureasil/As$_2$S$_3$ composite was obtained by mixing the ureasilicate monomer with the solution of chalcogenide clusters. The stiff gel was obtained as described above.

Chemical structures of the ureasil polymers used in the research are shown in Table 1 and their images are shown in Fig. 1.

The photocross-linked polymers ELO/RD was synthesized by the reaction of ELO (epoxidized linseed oil, having an average number of 6 epoxy groups per molecule) and RD (bisphenol A diglycidyl ether), using PI (50% mixture of triarylsulfonium hexafluorophosphate in propylene carbonate) as photoinitiator (Kavetskyy *et al.*, 2019). Chemical structures of the photocross-linked polymers used in the research are shown in Table 2.

The positron annihilation spectroscopy is suitable for characterizing the microstructure of investigated materials on the atomic and molecular scale (Goworek, 2014).

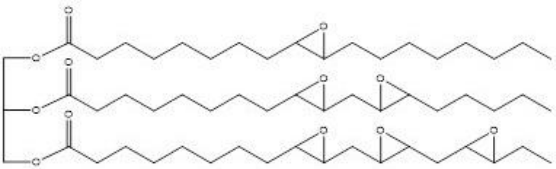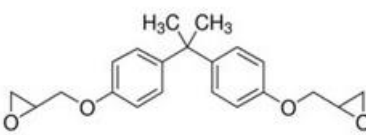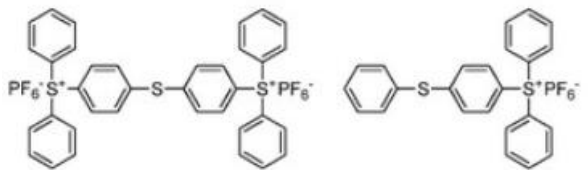**Table 1.** Chemical structures of the ureasil polymers used in the research

Samples	Materials and Formula
Ureasil	**Initial components:** - 3-(Triethoxysilyl)propyl isocyanate (ICPTES); - O,O′-Bis(2-aminopropyl) polypropylene glycol-block-polyethylene glycol-block-polypropylene glycol (Jeffamine ED-600). $a + c = 2.5, b = 8$
Ureasil/As$_2$S$_3$ composite	**Initial components:** - Triethoxy (3-isocyanatopropyl)silane (ICPTES); - O,O′-Bis(2-aminopropyl) polypropylene glycol-block-polyethylene glycol-block-polypropylene glycol (Jeffamine ED-600); - As$_2$S$_3$, dispersed in butylamine (CH$_3$(CH$_2$)$_3$NH$_2$). Colloidal solution of As$_2$S$_3$ in butylamine.
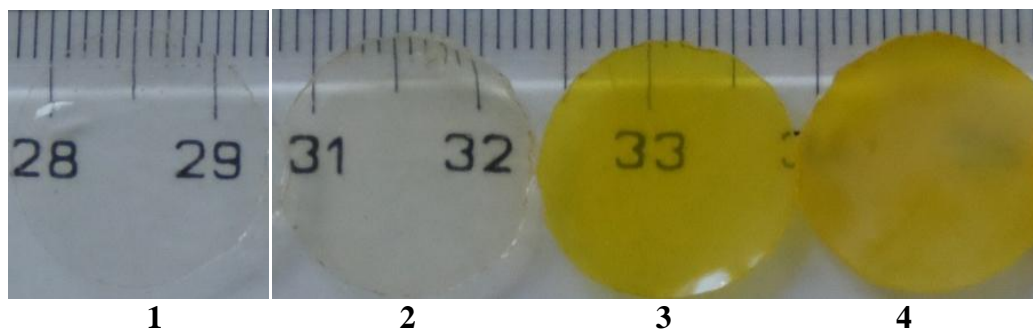
Fig. 1. Images of the investigated ureasil polymers used for the research (Kavetskyy *et al*., 2017a):
1 – ureasil fresh (2 months after preparation): 'K0-fresh';
2 – ureasil aged (1 year after preparation): 'K0-aged';
3 – ureasil/As_2S_3 fresh (2 months after preparation): 'K4-fresh';
4 – ureasil/As_2S_3 aged (1 year after preparation): 'K4-aged'

Table 2. Chemical structures of the photocross-linked polymers used in the research

Sample	Materials	Formula
ELO/RD	Epoxidized linseed oil	
	Bisphenol A diglycidyl ether	
	Triarylsulfonium hexafluoroantimonate salts (photoinitiator)	

The measurements of positron and positronium lifetime by the positron annihilation lifetime spectroscopy (PALS) spectrometer with the time resolution FWHM of ~220-320 ps cover the time range from 1 up to 142 ns. From the lifetimes the free-volume pore sizes (Tao, 1972; Eldrup *et al*., 1981) as well as their thermal expansion characteristics were determined. The spherical void size r_h was determined from the *ortho*-positronium (*o*-Ps) lifetime in the simple approach by the semi-empirical relation Eq. 1, where $\Delta R = 0.166$ nm is the empirical constant (Eldrup *et al*., 1981):

$$\tau_{o-Ps} = 0.5 \left\{ 1 - \frac{r_h}{(r_h + \Delta R)} + \left(\frac{1}{(2\pi)}\right) \sin\left[\frac{2\pi r_h}{(r_h + \Delta R)}\right] \right\}^{-1} \tag{1}$$

The corresponding hole volume V_h is given by equation:

$$V_h = \frac{4}{3} \pi r_h^3 \qquad (2)$$

The important characteristics as glass transition temperatures T_g (or temperatures of crystallization in some cases) and the coefficients for the thermal expansion of free-volume holes, $\alpha_F = 1/V_h(T_g^{PALS})(\Delta V_h/\Delta T)$ below (α_{F1}) and above (α_{F2}) T_g from $V_h(T)$ dependences were revealed.

Swelling method is suitable technique for the characterization of crosslinked systems. In the swelling experiment, the samples were immersed in suitable solvents at room temperature and weighted the initial weight (m_0) and final weight ($m_{swollen}$) after 8 days. Then the samples were dried at 333 K in argon atmosphere by using TGA method for obtaining the weight of dry sample (m_{dry}). The percent equilibrium mass swelling (S), the molecular weight between two crosslink points, M_c, was estimated by the Flory-Rehner equation as shown in (Kavetskyy *et al*., 2017a). The density of the investigated polymeric samples, $\rho_{polymer}$ was estimated by the gravimetric method (Archimedean principle).

3.   Results and discussion

Figure 2 shows the *o*-Ps lifetimes and their relative intensities for the investigated pure ureasil samples as a function of temperature in the range of 15-350 K (Kavetskyy *et al*., 2017a). The temperature where the free volume (*o*-Ps lifetime) changes slope is assigned as a glass transition temperature T_{g1}. The determined values of hole volume V_h (Eq. 2) at the glass transition temperature (T_{g1}) and the coefficients for the thermal expansion of free-volume holes α_{F1}, α_{F2} below and above T_{g1}, respectively, are gathered in Table 3. The lower temperature at which the slope of the $V_h(T)$ also changes in some cases is designated as T_{g2}.
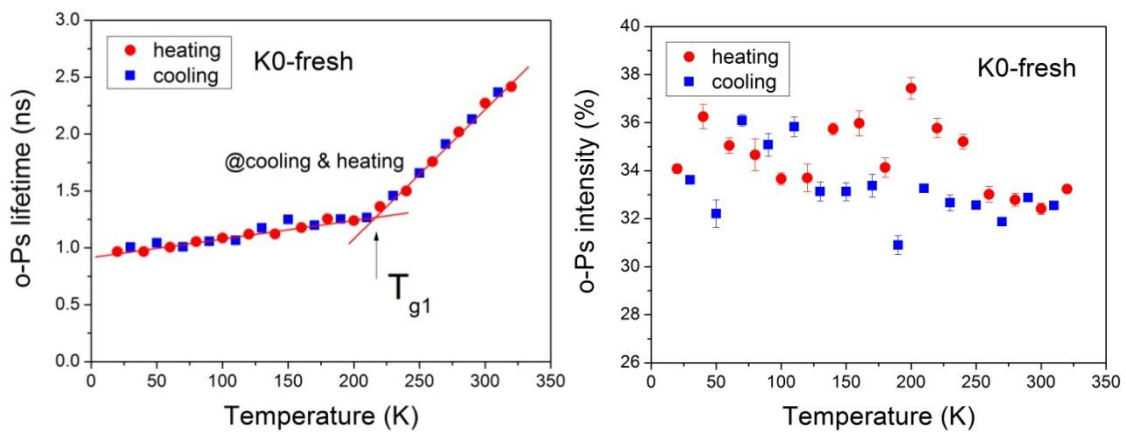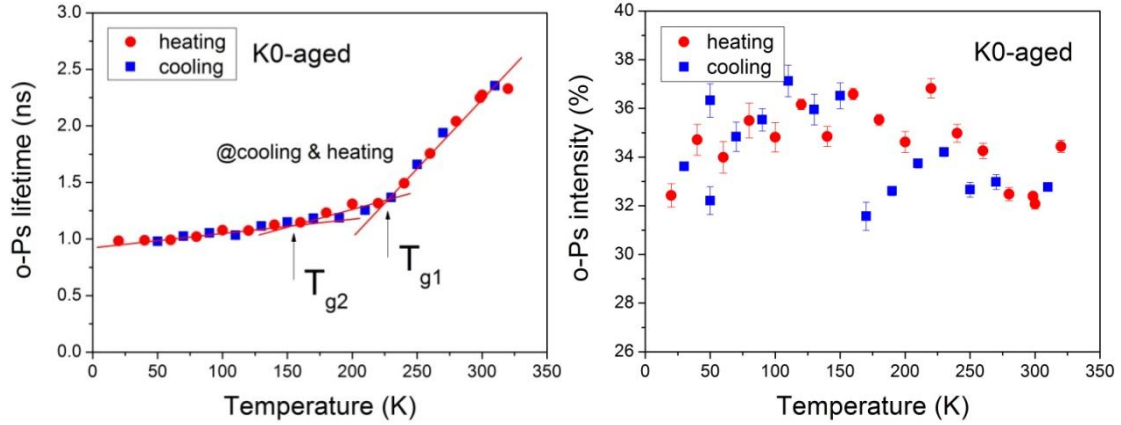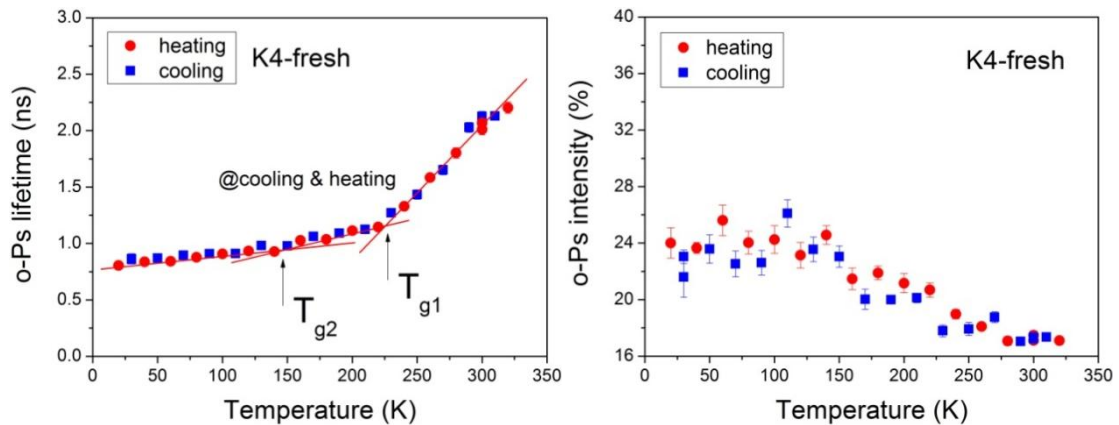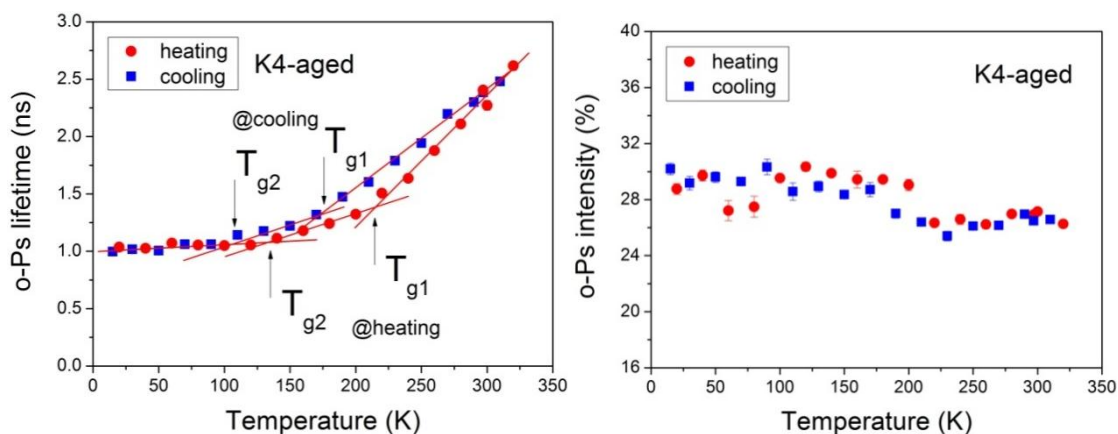
Fig. 2. *o*-Ps lifetime τ_3 (left) and intensity I_3 (right) as a function of temperature for the pure ureasil (K0) samples of this study. The error bars are within the size of the symbol. The solid lines are drawn as a guide for the eye. The samples are marked as shown in Fig. 1. Adapted from (Kavetskyy *et al.*, 2017a)

Table 3. Free-volume (V_{h1}) at glass transition temperature (T_{g1}), T_{g1}, lower temperature at which $V_h(T)$ changes the slope (T_{g2}) and the coefficients for the thermal expansion of free-volume holes α_{F1}, α_{F2} below and above T_{g1}, respectively, for the investigated ureasil polymers (Kavetskyy *et al.*, 2017a). The samples are marked as shown in Fig. 1

Sample	V_{h1} (nm^3)	T_{g1} (K)	T_{g2} (K)	$\alpha_{F1\ (T < Tg1)}$ (10^{-4} K^{-1})	$\alpha_{F2\ (T > Tg1)}$ (10^{-4} K^{-1})
K0-fresh (cooling & heating)	0.123 ± 0.002	216 ± 13	-	25 ± 3	286 ± 21
K0-aged (cooling & heating)	0.123 ± 0.003	230 ± 19	166 ± 89	53 ± 22	273 ± 99
K4-fresh (cooling & heating)	0.104 ± 0.001	227 ± 18	126 ± 38	48 ± 10	344 ± 63
K4-aged (cooling)	0.134 ± 0.001	178 ± 19	88 ± 58	46 ± 17	206 ± 56
K4-aged (heating)	0.123 ± 0.004	228 ± 38	130 ± 38	56 ± 22	237 ± 84

Figure 3 shows the *o*-Ps lifetimes and their relative intensities for the ureasil/As$_2$S$_3$ composite samples as a function of temperature in the range of 15-350 K (Kavetskyy *et al.*, 2017a). Both T_{g1} and T_{g2} are detected for both composites. In addition, it is found that the changes in hole volume depend on cooling or heating rate in the case of aged ureasil/As$_2$S$_3$ samples (K4-aged).

Fig. 3. *o*-Ps lifetime τ_3 (left) and intensity I_3 (right) as a function of temperature for the ureasil/As$_2$S$_3$ samples of this study. The error bars are within the size of the symbol. The solid lines are drawn as a guide for the eye. The samples are marked as shown in Fig. 1. Adapted from (Kavetskyy *et al*., 2017a)

The differences in network behavior for the aged samples and the effect of chalcogenide (As$_2$S$_3$) particles on the free volume of ureasil network are clearly observed, but further research is still needed to resolve the nature of double T_g values. Comparing the results presented in Table 3, it is seen that the largest changes in microscopical free volume characteristics represented by α_{F1} and α_{F2} are observed for the fresh ureasil/As$_2$S$_3$ sample (K4-fresh).

Figure 4 shows the swelling data for the investigated ureasil polymers (Kavetskyy *et al*., 2017a). Note, for the K4-fresh sample the largest changes in the swelling test parameters are also observed (Table 4). It is interesting to report here that the amperometric laccase-based biosensor constructed using K4-fresh polymer was characterized by the highest sensitivity compared with the pure K0-fresh one (Kavetskyy *et al*., 2018).
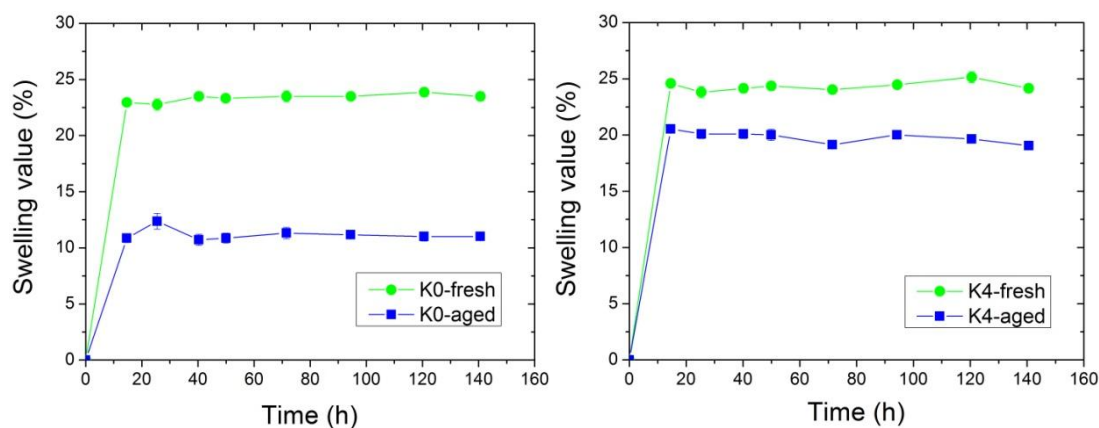
Fig. 4. The swelling values as a function of time for the pure ureasil (K0) samples (left) and the ureasil/As$_2$S$_3$ composite (K4) samples (right) of this study in EtOH at room temperature. The samples are marked as shown in Fig. 1. Adapted from (Kavetskyy *et al*., 2017a)

Table 4. Bulk density of the polymeric sample (ρ_p), molecular weight between two crosslink points (M_c) and comparative analysis of crosslinking density or swellability for the investigated polymers (Kavetskyy *et al*., 2017a). The samples are marked as shown in Fig. 1

Sample	ρ_p (g/cm^3)	M_c	Comparative analysis
K0-fresh	1.1778 ± 0.0021	92.47	lower crosslinking density, higher swellability
K0-aged	1.1814 ± 0.0012	44.0	the highest crosslinking density, the lowest swellability
K4-fresh	1.2015 ± 0.007	99.22	the lowest crosslinking density, the highest swellability
K4-aged	1.2170 ± 0.003	76.52	higher crosslinking density, lower swellability

Figure 5 shows the hole volume V_h calculated from *o*-Ps lifetimes and the *o*-Ps relative intensities for the investigated photocross-linked polymers ELO/10RD and ELO/30RD as a function of temperature in the range of 15-350 K (Kavetskyy *et al*., 2019). In both polymers, the changes in hole volume depend on cooling or heating rate.
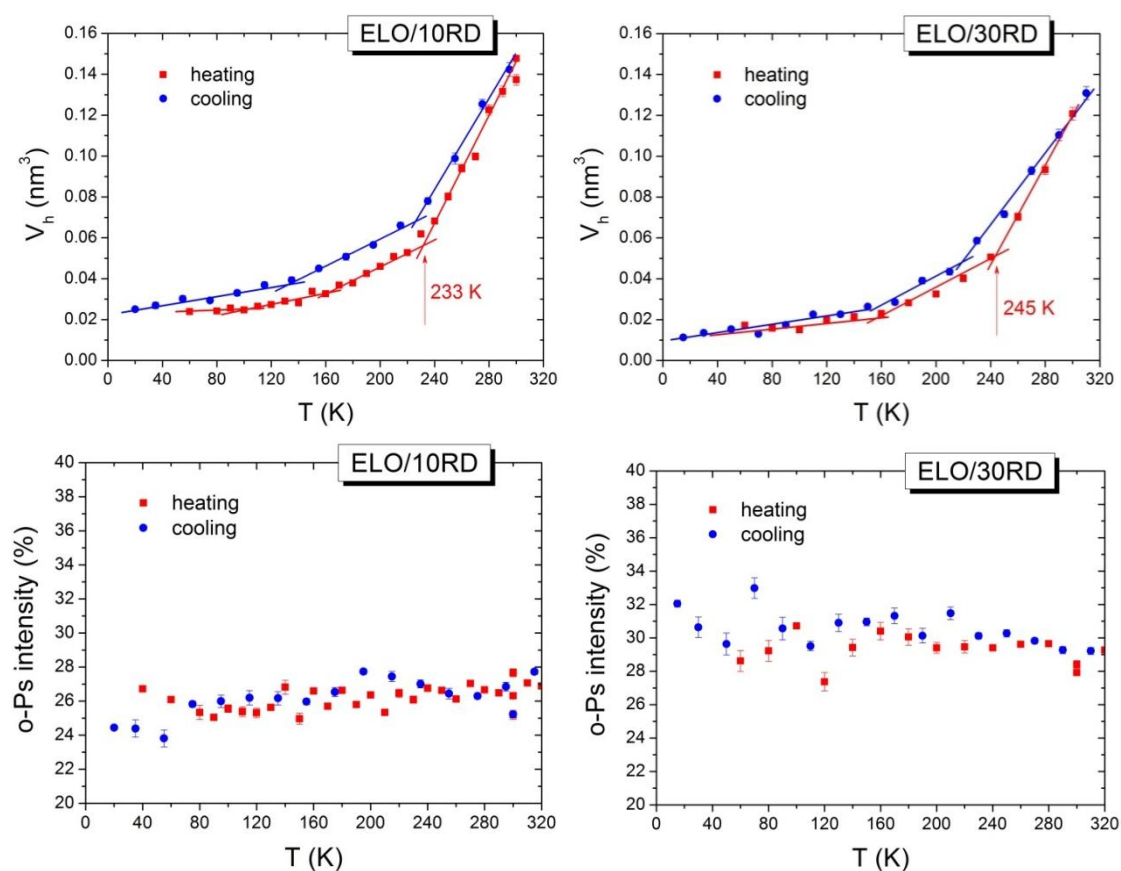
Fig. 5. Hole volume and *o*-Ps intensity temperature dependences for the photocross-linked polymers ELO/10RD (left) and ELO/30RD (right) in the heating and cooling cycles. Adapted from (Kavetskyy *et al*., 2019)

It can be noted that the average sizes of free-volume holes in the polymer ELO/10RD are larger than that of ELO/30RD. Also, the polymer ELO/10RD compared to the polymer ELO/30RD has the larger difference in the coefficients for the thermal expansion of free-volume holes in the regions below and above T_g (Table 5) (Kavetskyy *et al*., 2019).

Figure 6 shows the results of swelling test for the polymers ELO/10RD and ELO/30RD in the solvents EtOH and H_2O (Kavetskyy *et al*., 2019). The polymer

ELO/10RD compared to the polymer ELO/30RD has the higher crosslink density or lower swellability (Table 5). Like to previous case with ureasil polymers, it is interesting again to mention that the amperometric laccase-based biosensor constructed using ELO/10RD polymer shows the improved biosensor's parameters compared to ELO/30RD (Kavetskyy *et al*., 2019).
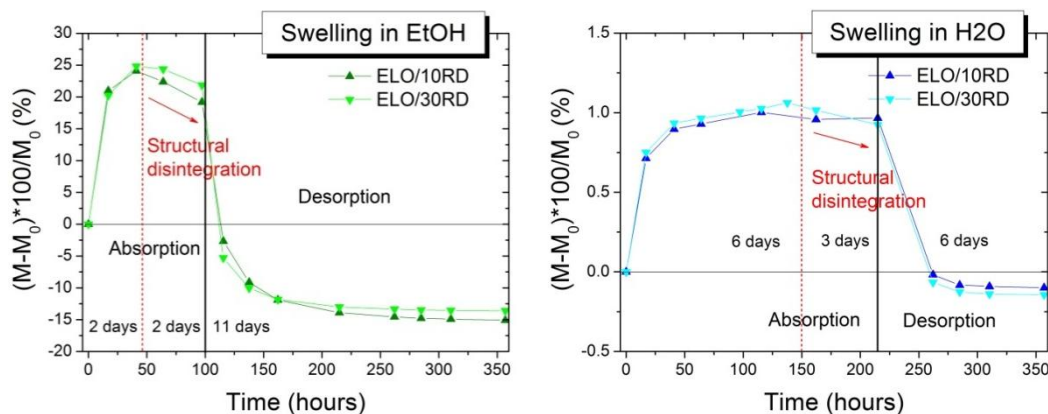
Fig. 6. The absorption and desorption of EtOH (left) and H_2O (right) of the polymers ELO/10RD and ELO/30RD during 15 days. Adapted from (Kavetskyy *et al*., 2019)

Table 5. Hole volume V_h at T_g, swellability S in EtOH, and slopes α_{F1}, α_{F2} of the $V_h(T)$ dependences in the regions below and above T_g, respectively, as well as their differences (values for heating and cooling cycles are in the top and bottom part of the boxes, respectively) (Kavetskyy *et al*., 2019)

Polymers	V_h (nm^3)	T_g (K)	S (%)	α_{F1} (10^{-4} K^{-1})	α_{F2} (10^{-4} K^{-1})	$\alpha_{F2} - \alpha_{F1}$ (10^{-4} K^{-1})
ELO/10RD	0.057 ± 0.002 0.068 ± 0.002	233	24.09	3.53 ± 0.30 3.31 ± 0.32	13.02 ± 0.60 11.16 ± 0.55	9.49 ± 0.67 7.85 ± 0.64
ELO/30RD	0.051 ± 0.002 0.049 ± 0.002	245	24.81	3.47 ± 0.33 3.87 ± 0.83	12.42 ± 0.64 8.96 ± 0.48	8.95 ± 0.72 5.09 ± 0.96

Therefore, for different kind of polymers used in this study, a correlation between the constructed biosensor parameters and microscopical free volume of the biosensor holding matrixes was established. It is foreseen that a change in microscopical free-volume below and above T_g represented by ($\alpha_{F2} - \alpha_{F1}$) in polymer matrix should be further tested as a possible control parameter for controlling the functionality of amperometric enzyme biosensor based on the polymer matrix.

4. Conclusions

Development of advanced materials for construction of biosensor with improved operational parameters is an important field in the novel sensor technologies. Novel polymer matrixes based on the organic-inorganic ureasil and ureasil/As_2S_3 composite were tested for immobilization of commercial microbial laccase and construction of amperometric biosensors (Kavetskyy *et al*., 2017a). A very high sensitivity of biosensor with ureasil/As_2S_3 composite was established and the positive effect of chalcogenide microparticles (MPs) on the biosensor's parameters was observed.

It was also established that the network properties of polymer matrix play a significant role for improvement of amperometric enzymatic biosensor but further

research is still needed to understand better the results obtained (Kavetskyy *et al*., 2018).

In the next step, the amperometric enzyme biosensors using photocross-linked polymers ELO/10RD and ELO/30RD as holding matrixes and immobilized commercial laccase from *Trametes versicolor* have been constructed on the surface of the graphite rods as working electrodes (Kavetskyy *et al*., 2019). It has been established that the application of the photocross-linked polymer ELO/10RD which is characterized by the higher crosslink density and larger free volume holes with their lower concentration and the larger change in microscopical free-volume below and above T_g compared to the polymer ELO/30RD results in the improvement of the laccase-based amperometric biosensor.

The larger change in microscopical free-volume below and above T_g was also detected for K4-fresh ureasil polymer which showed the most improved sensitivity of biosensor compared to K0-fresh ureasil used (Kavetskyy *et al*., 2018).

A change in microscopical free-volume below and above T_g represented by ($\alpha_{F2} - \alpha_{F1}$) in polymer matrix should be further tested as a possible control parameter for controlling the functionality of amperometric enzyme biosensor based on the polymer matrix. However, further research is still needed to prove the above correlation for other polymers with different crosslink density and/or morphology as well as to compare the operational parameters of the constructed biosensors with similar analogues known in literature.

Acknowledgments

References

Aravindakshan, J., Paquet, V., Gregory, M., Dufresne, J., Fournier, M., Marcogliese, D.J., Cyr, D.G. (2004). Consequences of xenoestrogen exposure on male reproductive function in spottail shiners (*Notropis hudsonius*). *Toxicological Sciences*, *78*, 156-165.

Arca-Ramos, A., Ammann, E.M., Gasser, C.A., Nastold, P., Eibes, G., Feijoo, G., Lema, J.M., Moreira, M.T., Corvini, P.F.-X. (2016). Assessing the use of nanoimmobilized laccases to remove micropollutants from wastewater. *Environmental Science and Pollution Research*, *23*, 3217-3228.

Boev, V., Pérez-Juste, J., Pastoriza-Santos, I., Silva, C.J.R., Gomes, M.J.M., Liz-Marzán, L.M. (2004). Flexible ureasil hybrids with tailored optical properties through doping with metal nanoparticles. *Langmuir*, *20*, 10268-10272.

Boev, V., Soloviev, A., Silva, C.J.R., Gomes, M.J.M. (2006). Incorporation of CdS nanoparticles from colloidal solution into optically clear ureasilicate matrix with preservation of quantum size effect. *Solid State Sciences*, *8*, 50-58.

Contardo-Jara, V., Lorenz, C., Pflugmacher, S., Nützmann, G., Kloas, W., Wiegand, C. (2011). Exposure to human pharmaceuticals Carbamazepine, Ibuprofen and Bezafibrate causes molecular effects in Dreissena polymorpha. *Aquatic Toxicology*, *105*, 428-437.

Danzo, B.J. (1998). The effects of environmental hormones on reproduction. *Cellular and Molecular Life Sciences*, *54*, 1249-1264.

Eldrup, M., Lightbody, D., Sherwood, J.N. (1981). The temperature dependence of positron lifetimes in solid pivalic acid, *Chemical Physics*, *63*, 51-58.

Giardina, P., Faraco, V., Pezzella, C., Piscitelli, A., Vanhulle, S., Sannia, G. (2010). Laccases: a never-ending story. *Cellular and Molecular Life Sciences*, *67*, 369-385.

Goworek, T. (2014). Positronium as a probe of small free volumes in crystals, polymers and porous media. *Annales Universitatis Mariae Curie-Sklodowska, Lublin-Polonia*, *69*, 1-109.

Kavetskyy, T., Lyadov, N., Valeev, V., Tsmots, V., Petkova, T., Boev, V., Petkov, P., Stepanov, A.L. (2012). New organic-inorganic hybrid ureasil-based polymer and glass-polymer composites with ion-implanted silver nanoparticles. *Physica Status Solidi C*, *9*, 2444-2447.

Kavetskyy, T., Šauša, O., Krištiak, J., Petkova, T., Petkov, P., Boev, V., Lyadov, N., Stepanov, A. (2013). New organic-inorganic hybrid ureasil-based polymer materials studied by PALS and SEM techniques. *Materials Science Forum*, *733*, 171-174.

Kavetskyy, T., Šauša, O., Čechová, K., Švajdlenková, H., Maťko, I., Petkova, T., Boev, V., Ilcheva, V., Smutok, O., Kukhazh, Y., Gonchar, M. (2017a). Network properties of ureasil-based polymer matrixes for construction of amperometric biosensors as probed by PALS and swelling experiments. *Acta Physica Polonica A*, *132*, 1515-1518.

Kavetskyy, T., Smutok, O., Demkiv, O., Kasetaite, S., Ostrauskaite, J., Švajdlenková, H., Šauša, O., Zubrytska, K., Hoivanovych, N., Gonchar, M. (2019). Dependence of operational parameters of laccase-based biosensors on structure of photocross-linked polymers as holding matrixes. *European Polymer Journal*, *115*, 391-398.

Kavetskyy, T., Smutok, O., Gonchar, M., Demkiv, O., Klepach, H., Kukhazh, Y., Šauša, O., Petkova, T., Boev, V., Ilcheva, V., Petkov, P., Stepanov, A.L. (2017b). Laccase-containing ureasil-polymer composite as the sensing layer of an amperometric biosensor. *Journal of Applied Polymer Science*, *134*, 45278(1-7).

Kavetskyy, T.S., Smutok, O., Gonchar, M., Šauša, O., Kukhazh, Y., Švajdlenková, H., Petkova, T., Boev, V., Ilcheva, V. (2018). Ureasil-based polymer matrices as sensitive layers for the construction of amperometric biosensors, in: Petkov, P., Tsiulyanu, D., Popov, C., Kulisch, W. (Eds.), *Advanced Nanotechnologies for Detection and Defence against CBRN Agents*, NATO Science for Peace and Security Series B: Physics and Biophysics, Dordrecht, Springer, 309-316.

Oehlmann, J., Schulte-Oehlmann, U. (2003). Endocrine disruption in invertebrates. *Pure and Applied Chemistry*, *75*, 2207-2218.

Patisaul, H.B., Adewale, H.B. (2009). Long-term effects of environmental endocrine disruptors on reproductive physiology and behavior. *Frontiers in Behavioral Neuroscience*, *3*, 10(1-18).

Roy, J.R., Chakraborty, S., Chakraborty, T.R. (2009). Estrogen-like endocrine disrupting chemicals affecting puberty in humans – a review. *Medical Science Monitor*, *15*, RA137-145.

Rozati, R., Reddy, P.P., Reddanna, P., Mujtaba, R. (2002). Role of environmental estrogens in the deterioration of male factor fertility. *Fertility and Sterility*, *78*, 1187-1194.

vom Saal, F.S., Hughes, C. (2005). An extensive new literature concerning low-dose effects of Bisphenol A shows the need for a new risk assessment. *Environmental Health Perspectives*, *113*, 926-933.

Sá Ferreira, R.A., Carlos, L.D., Gonçalves, R.R., Ribeiro, S.J.L., de Zea Bermudez, V. (2001). Energy-transfer mechanisms and emission quantum yields in Eu^{3+}-based siloxane-poly(oxyethylene) nanohybrids. *Chemistry of Materials*, *13*, 2991-2998.

Stathatos, E., Lianos, P., Stangar, U.L., Orel, B., Judeinstein, P. (2000). Structural study of hybrid organic/inorganic polymer gels using time-resolved fluorescence probing. *Langmuir*, *16*, 8672-8676.

Tao, S.J. (1972). Positronium annihilation in molecular substances, *The Journal of Chemical Physics*, *56*, 5499-5510.

Watson, C.S., Jeng, Y.J., Guptarak, J. (2011). Endocrine disruption via estrogen receptors that participate in nongenomic signaling pathways. *The Journal of Steroid Biochemistry and Molecular Biology*, *127*, 44-50.

de Zea Bermudez, V., Alcácer, L., Acosta, J.L., Morales, E. (1999). Synthesis and characterization of novel urethane cross-linked ormolytes for solid-state lithium batteries. *Solid State Ionics*, *116*, 197-209.

Zhou, Y., Wang, L., Liu, J., Li, W., Zheng, J. (2012). Options of sustainable groundwater development in Beijing Plain, China. *Physics and Chemistry of the Earth*, *47-48*, 99-113.